APPLIED ORGANOMETALLIC CHEMISTRY
Appl. Organometal. Chem. 2005; **19**: 750–758
Materials, Nanoscience and Catalysis AOC
Published online 18 March 2005 in Wiley InterScience (www.interscience.wiley.com). DOI:10.1002/aoc.887

Optimization of colloidal nanoparticle synthesis via $NR_4(BEt_3H)$ reduction

S. Kinge and H. Bönnemann*

Max-Planck-Institut für Kohlenforschung, Kaiser-Wilhelm Platz 1, Mülheim a. d. Ruhr D-45470, Germany

Received 8 November 2004; Revised 12 December 2004; Accepted 20 December 2004

Optimization of platinum and PtRu colloid syntheses via $NR_4(BEt_3H)$ reduction was achieved via the 'reverse addition mode'. The amount of stabilizing agent could be reduced by 40%. This improvement leads to a better particle size control and a considerable reduction of unwanted organic residues on the metal colloid particle surface. The PtRu catalyst prepared by reverse addition mode shows improvement in the methanol oxidation activity. Copyright © 2005 John Wiley & Sons, Ltd.

KEYWORDS: colloidal nanoparticle synthesis; reverse addition mode; fuel cell catalysts; methanol oxidation

INTRODUCTION

In last few decades a wealth of knowledge has been acquired about metallic colloidal materials.[1–5] Mono- and bi-metallic colloids can be used for the manufacturing of heterogeneous catalysts by the 'precursor concept'.[3–7] Further, the potentials of nanostructured metal colloids as fuel cell catalysts has been well evaluated.[8] Metal particles in the size range of 1–10 nm can be prepared in colloidal state by wet chemical reduction methods. In contrast to conventional impregnation or precipitation methods, these precursors may be tailored. Further, tetraalkylammonium hydrotriorganoborates as reductants[3–8] offer a wide range of applications in the wet chemical preparation of transition-metal colloids in organic solvents. The general pathway for this method is

$$MX_v + NR_4(BEt_3H) \longrightarrow M\text{–Colloid} + vNR_4X + vBEt_3 + v/2H_2\uparrow \quad (1)$$

M = metals of Groups 6–11; X = Cl, Br; $v = 1, 2, 3$; and R = alkyl, C_6–C_{20}. In it the reducing hydride species $[BEt_3H]^-$ is combined with the stabilizing agent NR_4^+ (R = alkyl, aryl, H groups). Consequently, the surface-active NR_4^+ groups are present immediately at the reduction centre in high local concentration, which effectively prevents particle aggregation. Trialkyl borane is recovered unchanged from the reaction and no borides contaminate the products. The resulting colloids are very stable and can be isolated in a high concentration, redispersed solid form. As synthesized, the NR_4^+-stabilized metal 'raw' colloids typically contain 6–12% of metal. 'Purified' transition-metal colloids containing 70–85% of metal are obtained by work-up with ethanol or diethyl ether and subsequent reprecipitation by a solvent of different polarity.

The preparative value of this method has been examined thoroughly previously.[3–8] In this study, an optimized version of this method is described. In NR_4Cl-stabilized colloids the interaction between the metal colloidal core and the chlorine atoms has been studied recently by Bönnemann and co-workers.[9] In NR_4Cl-stabilized colloids, NR_4Cl is anchored on the metal surface via chlorine atoms (Fig. 1).

In essence, X-ray absorption near-edge structure, metastable impact electron spectroscopy, and ultraviolet photoelectron spectroscopy studies have proved that not all of the NR_4Cl groups, compulsively liberated, as shown in Eqn (1), are bound to the colloidal metal surface, i.e. that there is an excess of protecting shell present in the colloidal solution. Usually, a 'conditioning step'[10] at higher temperatures has to follow to remove the unnecessary protecting agent, which can alter the properties of nanoparticles in an irreversible and non-controllable way.[11] Moreover, it was found that conditioning of NR_4Cl-stabilized colloidal catalysts leads to the contamination of the catalyst with chlorine impurities. Chloride anions are strongly adsorbed on platinum crystallites, which dramatically affects the kinetics of electro-catalytic reactions, e.g. oxidation of small organic molecules or oxygen reduction.[12]

*Correspondence to: H. Bönnemann, Max-Planck-Institut für Kohlenforschung, Kaiser-Wilhelm Platz 1, Mülheim a. d. Ruhr D-45470, Germany.
E-mail: boennemann@mpi-muelheim.mpg.de; helmut.boennemann@itc-cpv.fzk.de
Contract/grant sponsor: Deutsche Forschungsgemeinschaft; Contract/grant number: BO 1135/2-5.

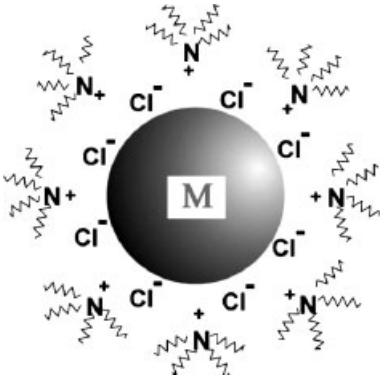

Figure 1. Scheme for the stabilization of the metal core by NR_4Cl as discussed in Ref.9.

Thus, the presence of chloride lowers the catalytic activity of proton exchange membrane fuel cell catalysts prepared from these colloidal precursors. This prompted us to reduce the amount of stabilizing agent as much as possible without altering the stability of the colloids. A further limitation of this method resides in the fact that particle sizes cannot be varied by altering the reaction conditions.

OPTIMIZATION SCHEME AND REVERSE ADDITION MODE

Optimization scheme

In the following experiments, optimization of the $NR_4(BEt_3H)$ reduction method was performed in order to minimize the amount of protecting agent (NR_4Cl). A variety Pt–$N(Octyl)_4Cl$, colloids were prepared with decreasing amounts of stabilizing $N(Octyl)_4Cl$. The stochiometrically balanced reaction for a typical $(Octyl)_4N[BEt_3H]$ synthesis of platinum colloid is

$$PtCl_2 + 2(Octyl)_4N(BEt_3H)(100\%) \longrightarrow Pt_{colloid}\,(\mathbf{1}) + 2(Octyl)_4NCl + 2BEt_3 + H_2\uparrow \quad (2)$$

In a series of experiments, the quantity $2\times(Octyl)_4N(BEt_3H)$ (given in Eqn (2)) was decreased in a stepwise manner to 80, 60, 40 and 20%. The necessary amount of reducing hydride was substituted by $LiBEt_3H$. The subsequent balanced equations are

$$PtCl_2 + 8/5(Octyl)_4N(BEt_3H)(80\%) + 2/5LiBEt_3H \longrightarrow Pt_{colloid}\,(\mathbf{2}) + 8/5(Octyl)_4NCl + 2/5LiCl + 2BEt_3 + H_2\uparrow \quad (3)$$

$$PtCl_2 + 6/5(Octyl)_4N(BEt_3H)(60\%) + 4/5LiBEt_3H \longrightarrow Pt_{colloid}\,(\mathbf{3}) + 6/5(Octyl)_4NCl + 4/5LiCl + 2BEt_3 + H_2\uparrow \quad (4)$$

$$PtCl_2 + 4/5(Octyl)_4N(BEt_3H)(40\%) + 6/5LiBEt_3H \longrightarrow Pt_{colloid}\,(\mathbf{4}) + 4/5(Octyl)_4NCl + 6/5LiCl + 2BEt_3 + H_2\uparrow \quad (5)$$

$$PtCl_2 + 2/5(Octyl)_4N(BEt_3H)(20\%) + 8/5LiBEt_3H \longrightarrow Pt_{colloid}\,(\mathbf{5}) + 2/5(Octyl)_4NCl + 8/5LiCl + 2BEt_3 + H_2\uparrow \quad (6)$$

The resulting colloids were then characterized by elemental analysis and transmission electron microscopy (TEM).

In order to produce fuel cell catalysts, these colloids were supported, conditioned on Vulcan XC 72 support and further characterized with X-ray diffraction (XRD) and BET analyses.

'Reverse addition mode' for particle size control

The 'reverse addition mode' was investigated to check the particle size control during $R_4N(BEt_3H)$ reduction. Normally, the reducing agent and the protecting shell mixture is added slowly to the metal salts solution, whereas in the 'reverse addition mode' this step is reversed, by adding the metal salts solution to the reducing agent–protecting agent [$R_4N(BEt_3H)$] solution.

In the $R_4N(BEt_3H)$ reduction method, nuclei are supposed to be generated instantaneously due to the strong reducing character of [BEt_3H^-].[13] In the usual mode, as the hydride addition is a slower process, the nuclei would be produced in subsequent steps of hydride addition. Consequently, diffusional growth is not favoured.[14] This could lead to a broad particle size distribution. Moreover, in the usual mode the presence of the dispersed metal salt ($PtCl_2$ is partially soluble in tetrahydroforan (THF)) could give an inhomogeneous environment for nanoparticle growth. In the case of the reverse addition mode, however, the rapid addition of a small fraction of platinum salt in the reducing–stabilizing agent is initially followed, where the immediately generated nuclei are stabilized and uniformly dispersed in the solution. This will give a homogeneous environment for diffusional nanoparticle growth.

To check the validity of the new reverse addition mode, the following experiments were set up. Colloids **6** and **7** were prepared as shown by balanced Eqns (7) and (8). Colloid **6** was prepared by reverse addition of $PtCl_2$ dispersed in THF, in $2(Octyl)_4N(BEt_3H)$. In the case of colloid **7**, $PtCl_2$ solution was added to a 1 : 1 molar mixture of $(Octyl)_4N(BEt_3H)$ and $LiBEt_3H$. Similar to the previous section, in this case the protecting agent was quantitatively reduced to 60% and the required reductant is substituted by $LiBEt_3H$.

$$2(Octyl)_4N(BEt_3H) + PtCl_2 \longrightarrow Pt_{colloid}(\mathbf{6}) + 2(Octyl)_4NCl + 2BEt_3 + H_2\uparrow \quad (7)$$

$$6/5(Octyl)_4N(BEt_3H) + 4/5LiBEt_3H + PtCl_2 \longrightarrow Pt_{colloid}(\mathbf{7}) + 6/5(Octyl)_4NCl + 4/5LiCl + 2BEt_3 + H_2\uparrow \quad (8)$$

Further, the co-reduction of transition-metal salts in solution with $(Octyl)_4N(BEt_3H)$ is the most widely used method to generate bimetallic colloidal suspensions.[15–19] Reproducible synthesis of PtRu colloids (~2 nm) with a very narrow particle size distribution is feasible.[19,20] This method is appropriate for preparing bimetallic colloidal catalysts for fuel cell electrodes and has been studied intensively.[21] In this study, a PtRu–NR_4Cl organosol was prepared subsequently. The balanced equation for the synthesis of colloidal PtRu-sol using tetraoctylammonium triethylhydroborate is

$$PtCl_2 + RuCl_3 + 5NR_4(BEt_3H) \longrightarrow Pt_{50}Ru_{50\ colloid}(\mathbf{8}) + 5NR_4Cl + 5BEt_3 + 5/2H_2\uparrow \quad (9)$$

Moreover, to extend the reverse addition mode concept to the PtRu colloid synthesis, PtRu colloids were prepared by the reverse addition mode as follows:

$$5(Octyl)_4N(BEt_3H) + PtCl_2 + RuCl_3 \longrightarrow Pt_1Ru_{1colloid}(\mathbf{9}) + 5(Octyl)_4NCl + 5BEt_3 + 5/2H_2\uparrow \quad (10)$$

$$2(Octyl)_4N(BEt_3H) + 3LiBEt_3H + PtCl_2 + RuCl_3 \longrightarrow Pt_1Ru_{1colloid}(\mathbf{10}) + 3(Octyl)_4NCl + 2BEt_3 + H_2\uparrow \quad (11)$$

These colloids were supported on Vulcan XC 72 and conditioned. They were termed **cat. 8–10**. The PtRu bimetallics were compared using TEM and XRD analysis and tested electrochemically.

EXPERIMENTAL

All the reactants and the products in this study are air sensitive. Therefore, all reactions were done under argon using Schlenk techniques. The vacuum utilized was 10^{-3} mb. All reactions are performed with distilled solvents.

Materials

$LiBEt_3H$ synthesis and $(Octyl)_4N[BEt_3H]$ synthesis are as described previously.[22] $PtCl_2$ and $RuCl_3$ were utilized as obtained from Aldrich chemicals.

Measurements

TEM

The colloidal sols were investigated using a Hitachi HF 2000 transmission electron microscope operating at 200 keV. The instrument is equipped with a cold field-emission source of tunssten(310) and capable of energy dispersive X-ray analysis (EDX). The objective lens was a high-resolution/analytical type (15° specimen tilt) with a spherical aberration coefficient of 1.2 mm, giving a point resolution of 0.23 nm and an information limit of 0.16 nm. The microscope was fitted with a Voyager 1000/S EDX system with a high take-off angle geometry of 68°, 0.037 sr solid angle and energy resolution for manganese of 140–143 eV. Spots as small as about 4 nm in diameter were analysed in the present study (which allows the identification of bimetallic structures). The samples were supported on a 6 nm thickness carbon film mounted on a copper grid.

XRD

XRD analysis was undertaken using a Siemens Typ, D500, using Cu Kα radiation with wavelength 1.54 Å. During this work the phase identification and the determination of the unit cell parameter was performed from the data measured with a STOE STADI P transmission diffractometer in Debye–Scherrer geometry with a primary monochromator of curved germanium (111) and a linear position sensitive detector. Cu Kα_1: 1.540 60 Å radiation is used. The data are collected mostly in the 2θ range between 15 and 90°, with a 2θ step width of 0.01°, counting time dependent on data quality.

BET

Surface area analysis was done using a Micrometrics ASAP 2010 chemisorption system

Electrochemistry

Linear sweep voltammograms for methanol oxidation were collected with EG&G Princeton applied research unit (Model 636), with a rotating disk electrode system. Methanol oxidation curves were obtained in a thermostated, standard three-compartment electrochemical cell. 0.5 M sulfuric acid is used as electrolyte (Merck suprapure). The methanol concentration used was 0.5 M. Potentials were measured against a mercury sulfate reference electrode. A glassy carbon disk electrode (Sigradur G from Hochtempperature Werkstoffe GmbH) with 6 mm diameter (0.283 cm^2), polished to a mirror finish (0.05 μm alumina, Buehler) before each experiment, was used as a substrate for Vulcan-supported catalysts. For the electrode preparation, a suspension of 2.5 mg ml^{-1} Vulcan catalysts in Millipore water were redispersed ultrasonically for about 10 min. A 20 μl aliquot was immediately, pipetted on to the surface of the glassy carbon disk electrode. After evaporation of the water under argon, the electrode surface was covered with 20 μl of Nafion solution in order to attach the Vulcan particles on the glassy carbon electrode, after evaporating again in a mild stream of argon. This gives a catalyst layer thickness on the order of less than 2 μm. The resulting Nafion film thickness of about 0.2 μm is of sufficient strength to permanently attach the catalyst particles to the glassy carbon electrode. Diffusion effects are negligible under these conditions.

Immediately after preparation the electrodes were immersed under potential control in the deaerated electrolyte (argon, N 6.0, Messer-Griesheim) at 0.1 V. Linear sweep voltammograms were obtained with a scanning rate of 50 mV s^{-1}.

Preparation of colloids and catalysts

*Pt-colloid **1** and catalyst **1***

2.5 g of $PtCl_2$ was suspended in 1 l THF. Then a solution of 120 ml of 0.19 M $(C_8H_{17})_4N[BEt_3H]$ in THF was added over

a span of 16 h. This instilling was done with the reducing agent in suspension to ensure complete reduction. Reduction is easily judged by the colour change from suspension to a dark-brown solution. After complete addition of reducing agent, 20 ml acetone was added to quench the reaction, and to destroy excess reducing agent. After drying *in vacuo* for 4 h at 40 °C, 17.2 g of colloid in form of a waxy, deep-black residue was obtained. 200 ml ethanol and 200 ml technical diethyl ether was added to wash the compound. Cleaning was repeated with 100 ml of distilled diethyl ether and 100 ml of distilled ethanol. Colloid **1** is very soluble in THF, toluene, acetone, ether and is insoluble in ethanol and pentane.

About 200 mg of this Pt-organosol **1** was stirred with 800 mg of Vulcan XC 72 in THF for 12 h. The solvent was then pumped off. A black, free-flowing powder was obtained as the residue. Conditioning of the supported colloid is a crucial step in which the removal of excess of protecting shell takes place thereby leaving metallic colloidal nanocrystallites dispersed on carbon black. The details of this step are mentioned elsewhere. Conditioning is done in 2% O_2(5) in Ar(4.5) (Messer Ltd), followed by H_2(5). The temperature was maintained at 300 °C, for 30 min each. The product is termed **cat. 1**.

*Pt-colloid **2** and catalyst **2***

2.5 g of $PtCl_2$ was dried *in vacuo*, suspended in 1 l THF, and stirred for 2 h. A mixture of reducing agents, 79.04 ml (0.19 M in THF) $(Octyl)_4N[BEt_3H]$ and 2.4 ml (1.63 M in THF) $LiBEt_3H$, was added dropwise over a period of 5 h. The solvent was pumped off, and the residue dried *in vacuo* to give a free-flowing black powder. 200 ml ethanol and 200 ml technical diethyl ether were added to wash the compound. Cleaning was repeated with 100 ml of distilled diethyl ether and 100 ml of distilled ethanol. Drying was carried out *in vacuo* and a free-flowing black powder obtained that was soluble in THF, toluene, and diethyl ether. This was subsequently supported on Vulcan and conditioned to give catalyst **cat. 2**.

*Pt-colloids **3**–**5** and catalysts **3**–**5***

The preparation steps were similar to **1** and **2**, but the quantities varied. The amounts of $NR_4(BEt_3H)$ were reduced to the required percentages and the balance replaced by $LiBEt_3H$, as shown in Eqns (3) to (5). The quantities applied during these syntheses are given in Table 1. The respective colloids and catalysts are termed **3**, **4**, and **5**.

*Pt-colloid **6***

The reverse addition mode of $PtCl_2$ in $(Octyl)_4N[BEt_3H]$ was followed. A suspension of 2.5 g $PtCl_2$ in THF 500 ml was added dropwise to the 120 ml reductant over a period of 12 h.

*Pt-colloid **7***

The reverse addition mode of $PtCl_2$ in $(Octyl)_4N[BEt_3H]$ was followed. A suspension of 2.5 g $PtCl_2$ in THF 500 ml was added dropwise to 83 ml $(Octyl)_4NBEt_3H$ and 6.5 ml of $LiBEt_3H$ reductant over a period of 12 h.

Table 1. Quantitative presentation of reactants applied during the synthesis of colloids **3**, **4**, **5**

Colloids	$PtCl_2$	$(Octyl)_4NBEt_3H$ (0.19 M/THF)	$LiBEt_3H$ (1.63 M/THF)	THF
3	3.5 g	83 ml	6.5 ml	1 l
4	3.5 g	55 ml	9.7 ml	1 l
5	3.5 g	28 ml	13.1 ml	1 l

*PtRu-colloid **8***

2.25 g of $PtCl_2$ and 1.752 g of $RuCl_3$ dried in vacuum were mixed and suspended in 1.5 l THF under argon. 213 ml of 0.19 M $(C_8H_{17})_4N[BEt_3H]$ in THF was added over 12 h at 40 °C. A nearly clear solution is obtained. To quench the reaction and destroy the reducing agent, 10 ml acetone was added. The solution was filtered under argon and evaporated. Drying for 16 h at 60 °C yielded a waxy, black residue. The colloid was very soluble in THF and toluene.

Elemental analysis shows platinum and ruthenium in 1 : 1 molar proportion.

The supported and conditioned catalyst is termed as **cat. 8**

*PtRu-colloid **9***

The reverse addition mode of metal salts in $(C_8H_{17})_4N[BEt_3H]$ was followed. Quantities were similar to previous syntheses.

*PtRu-colloid **10***

The reverse addition mode of metal salts in $(C_8H_{17})_4N[BEt_3H]$ and $LiBEt_3H$ solution was followed. In this case the amount of $(C_8H_{17})_4N[BEt_3H]$ (158 ml) is reduced to half as used in colloid **9** synthesis and half of the reducing agent was replaced by $LiBEt_3H$ (14.2 mmol).

The catalyst prepared from colloid **10** is termed **cat. 10**. Elemental analysis showed platinum and ruthenium in 1 : 1 molar proportion.

RESULTS AND DISCUSSION

The colloids **1**, **2** and **3** were obtained as waxy, black residues. The resulting colloids were highly soluble in THF, toluene, and diethyl ether, but insoluble in ethanol and pentane. After washing, the colloids **1** and **2** were readily soluble in THF, and colloid **3** was dispersible in THF to a smaller extent. In the case of colloids **4** and **5** the particles settle down immediately after reduction and acetone quenching, with a clear supernatant solution. This suggests that colloids **4** and **5** did not contain sufficient amounts of protecting agent, resulting in non-redispersible particles. TEM comparison of the particle sizes and elemental analysis of the colloids were

Table 2. BET surface area and elemental analysis

Colloid or catalyst (Protective shell (%))	Pt (colloid) content (%)	Catalyst BET surface area ($m^2\ g^{-1}$)
1 (100)	78	195
2 (80)	85	190
3 (60)	93.25	178
4 (40)	97	168

correct out, and BET and XRD studies were done for all catalysts. See Table 2.

The catalysts (**cat. 1** to **cat. 4**) prepared were free-flowing, shining, black powders.[12] During the conditioning step, the protective shell was largely removed to a give metallic lustre, indicating clean nanoparticle surfaces.[15–17] All catalysts show very high BET surface areas. BET surface area is a measure of the available surface for catalysis. The BET surface area and elemental analysis results are presented in Table 2. All representative TEM results are shown in Fig. 2. All colloids show similar particle size distributions. A typical representative high-resolution TEM image at 5 nm scale is shown for colloid **1** in Fig. 2e. Particles of average size 3–4 nm are visible. All other colloids show similar particle sizes. Dried colloid **1** and colloid **4** powders were investigated by powder XRD. The lattice parameters were determined as ~3.92 Å in both cases, which is identical with the theoretical value of pure platinum, and the different lattice planes were assigned (Fig. 3). Particle sizes were determined using these data and the Scherrer equation and found to be 4–5 nm.

Therefore, it is clear from the TEM and XRD analyses that the particle size distributions of these different colloidal catalysts are almost identical. Thus, the amount of protecting agent can be reduced by ~40% without changes in particle size distribution. Though colloid **4** has a similar particle size (Fig. 2d) to other colloids (Fig. 2a–c), it is not suitable for catalyst preparation because insoluble particulates settle down immediately after the reduction. TEM (Fig. 2d) shows the dispersed part of the colloid only. From this comparison it can be concluded that 60% of the stabilizing NR_4Cl (Eqn (4)) is the minimum needed to give a fully redispersible Pt-colloid. This, in turn, means that 40% of the NR_4Cl can be saved.

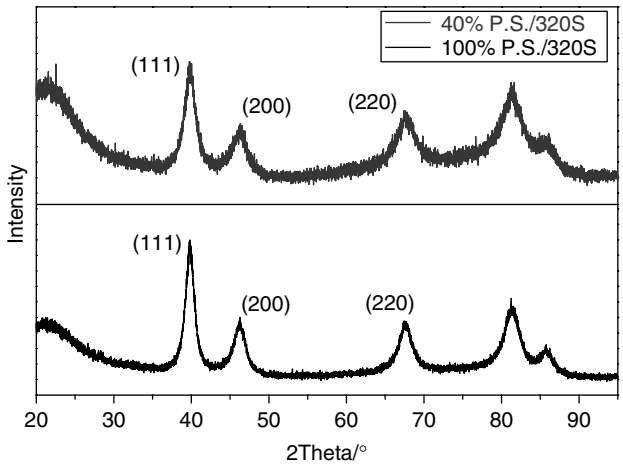

Figure 3. XRD of (a) **cat. 4** and (b) **cat. 1**.

All in all, it can be concluded that less than 60% of stabilizing shell gives non-dispersible platinum nanopowders. And one can indeed decrease the amount of NR_4Cl protective shell for colloidal platinum synthesis to 60%.

Reverse addition mode

It is interesting to note that neither the size nor the morphology of the particles can be altered by changing the amount of tetraalkylammonium stabilizer applied in the *in*

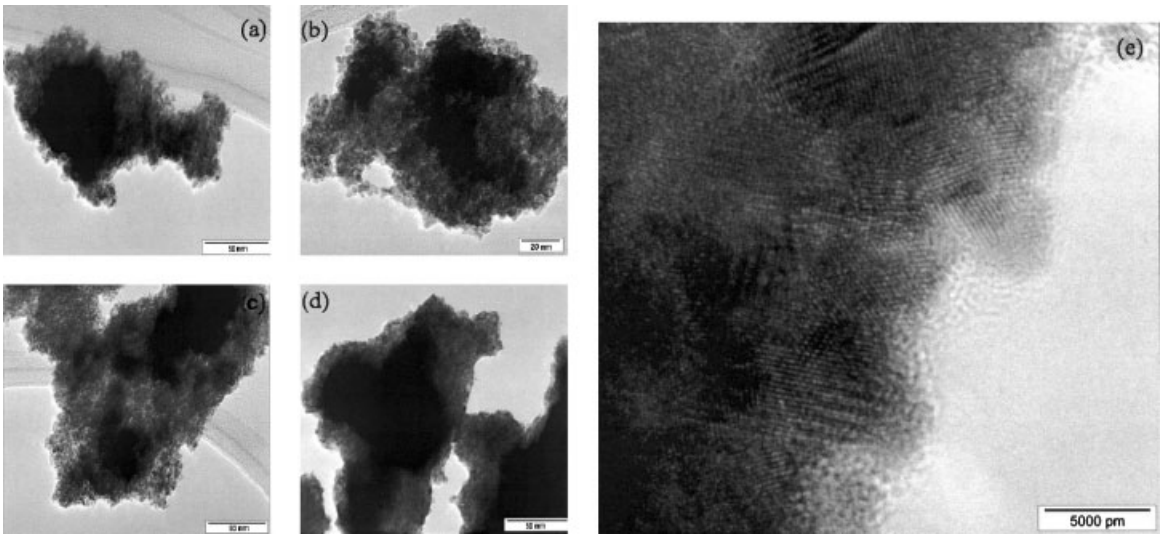

Figure 2. (a) TEM of colloid **1**; (b) TEM of colloid **2**; (c) TEM of colloid **3**; (d) TEM of colloid **4**; (e) high-resolution TEM of colloid **1**.

situ reduction mode.[17] In the reverse addition mode (Eqns (6) and (7)), however, diffusional growth is expected to lead to uniform particle sizes and so unwanted aggregation of the platinum particles can be avoided. In contrast, diffusional growth is less feasible when a large number of nuclei are generated simultaneously in reduction. In the usual reduction pathway, smaller particles are formed which would then aggregate further.[13,14] Thus, the reverse addition method is advantageous, as the creation of an identical environment for nanoparticle growth is feasible. Additionally, if the initial batch of salts is added rapidly, then a sufficiently large number of nuclei will be generated and when the next batch is slowly added the resulting particles will lead to more uniformity.

TEM analysis showed that the reverse addition indeed yields smaller particles with a narrow particle size distribution. The particle size distributions of both colloids **6** (1.9 nm) and **7** (2.5 nm) were found to be similar (Fig. 4).

The size and shape of the final nanoparticles vary depending upon the initial concentration of nuclei and reduction rate. When a solution of $(Octyl)_4N(BEt_3H)$ is added to the metal salt suspension the nuclei formed are not homogeneously dispersed because the local $(Octyl)_4NCl$ concentration is too low. Subsequently, the nuclei formed will not be in immediate contact with the initially formed nuclei due to inhomogeneous conditions. This gives rise to unwanted particle growth.

In the reverse addition mode, all the nuclei formed are immediately stabilized with the protecting agent and dispersed homogeneously in the solution. Thus, the reverse addition mode favours the formation of a homogeneous particle size distribution via growth control. Further, the particle size was found to be dependent on the amount of stabilizer. For a 100% stabilizing shell the particles were smaller, on average being 1.9 nm, whereas when a 50% amount was used they were 2.5 nm. This can be rationalized based on the assumption that a greater amount of protecting agent hinders particle growth to a larger extent. But this is a very small difference and difficult to conclude.

PtRu particles

The bimetallic PtRu colloid (**8**) was examined by TEM (see Fig. 5). The average diameter is 1.8 nm with a standard deviation of 0.5 nm. The composition of PtRu clusters was investigated by point-resolved EDX, yielding 55% platinum and 45% ruthenium. Thus, the single particle composition is nearer to the expected mixture of $Pt_{50}Ru_{50}$, which confirms homogeneous alloying of the platinum and mithenium. Thus, this sample could used directly be as a fuel cell catalyst.[21]

Powder XRD of **cat. 8** reveals sharp reflections on top of very broad ones. Sharp reflections correspond to platinum particles grown in size. From the high-temperature *in situ* measurement up to 500 °C, the analysis of the peaks gives a lattice parameter corresponding to PtRu alloyed particles (3.89 nm) (Fig. 5c). Average particle size after conditioning of PtRu particles is 3–4 nm, indicating particle growth during the conditioning step. Thus, very high surface area catalysts can be prepared by this method.

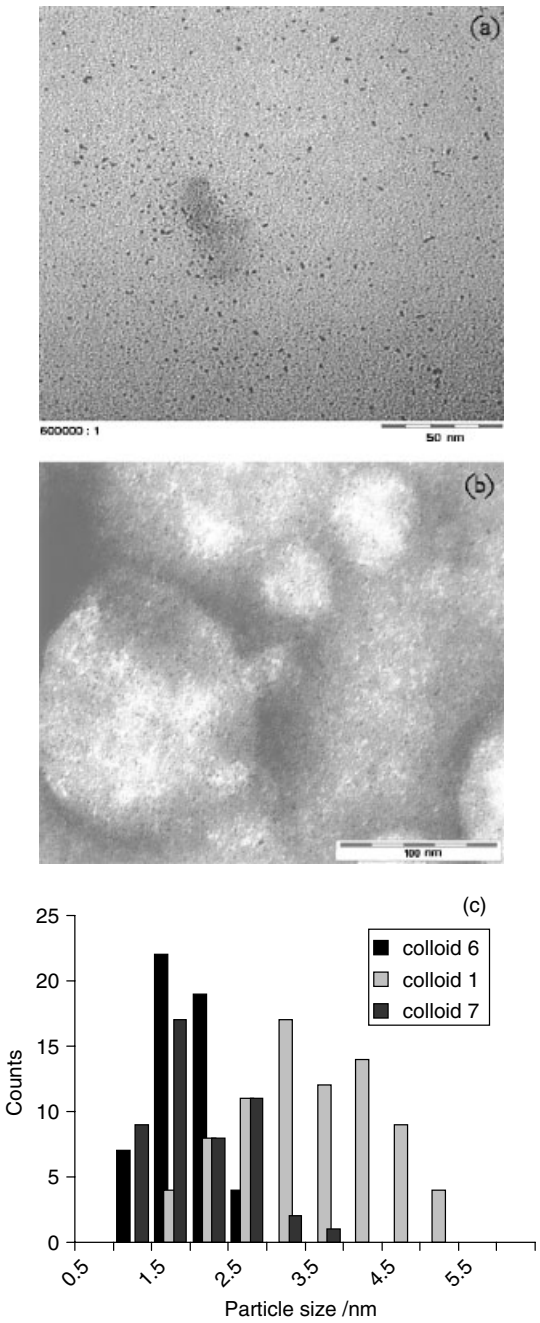

Figure 4. TEM analyses for colloids by reverse addition mode: (a) colloid **6**, average particle size 1.9 nm; (b) colloid **7**, average particle size 2.5 nm. (c) Particle size distribution.

The optimum amount of NR_4X required for PtRu colloid stabilization

By following the reverse addition mode the colloids **9** and **10** obtained were homogeneous and redispersible in THF. TEM analysis results indicate that the average particle size

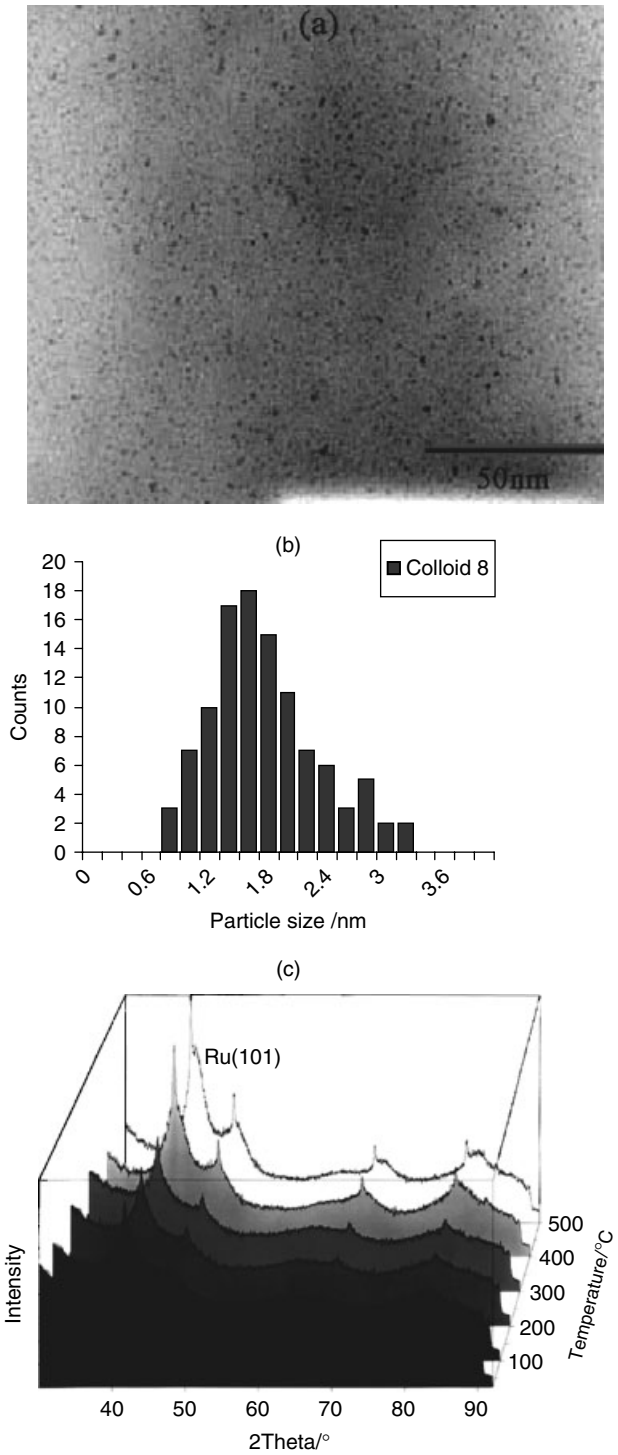

Figure 5. (a) TEM of colloid **8**; (b) particle size distribution; (c) high-temperature XRD analysis of **cat. 8**.

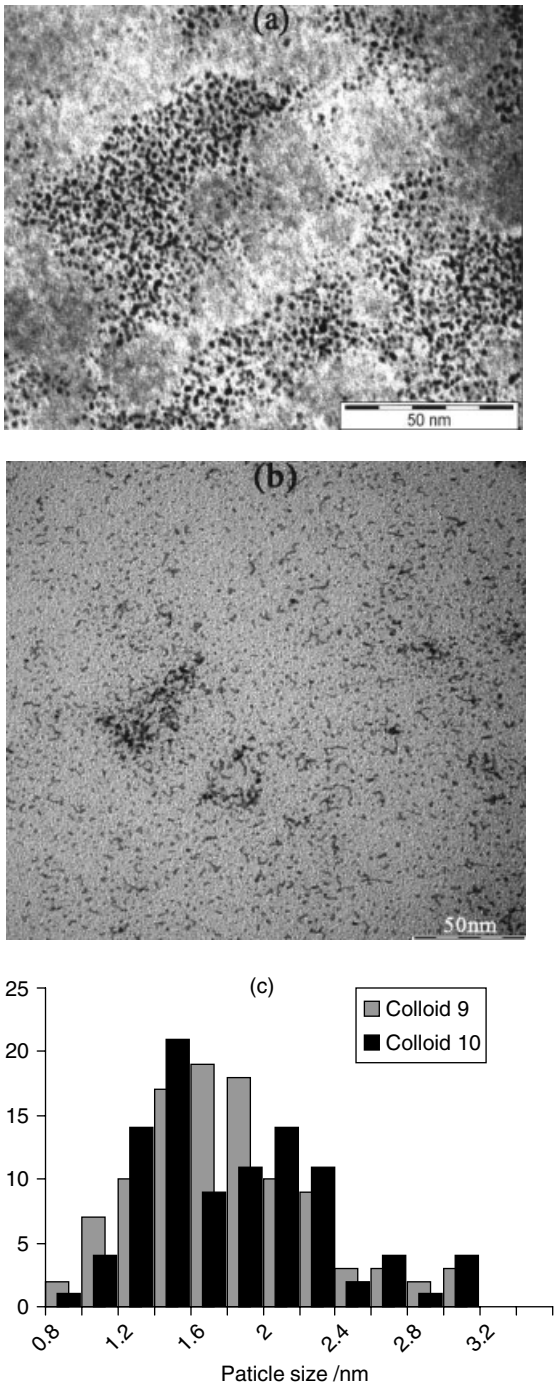

Figure 6. TEM analysis of (a) colloid **9** and (b) colloid **10**. (c) Particle size distribution.

remains unchanged in both cases. The average particle size changes from 1.9 nm for **10** to 2.2 nm for **9** (Fig. 6; compared with 1.8 nm for colloid **8**). Thus, in the case of PtRu colloid, one can indeed reduce the amount of tetraalkylammonium protective shell to 60% using this reverse addition mode. There is little change in the particle size using this mode. A pictorial presentation of reverse addition mode of PtRu-colloid synthesis is given in Fig. 7.

Methanol oxidation of catalysts cat. 10 and cat. 8

The study of the reverse addition mode finds that the particle size distribution of the resulting colloids **8** and **10** remains

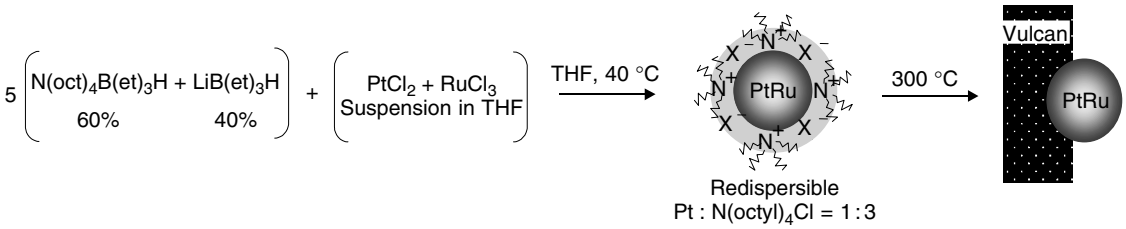

Figure 7. Pictorial presentation of reverse addition mode PtRu-colloid synthesis.

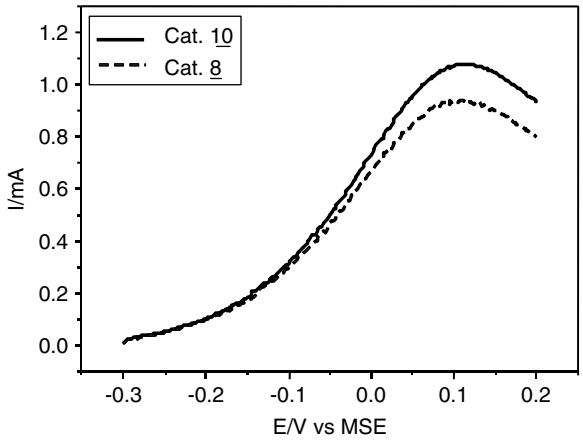

Figure 8. Methanol oxidation of **cat. 8** and **cat. 10**, at 50 mV s^{-1} scan rate.

almost the same compared with tetraalkylammonium borate-based method, but the advantages are lower costs and less impurities generated. Methanol oxidation current densities at a 50 mV s^{-1} scan rate of catalyst **10** were compared with PtRu-catalyst **8**. It was found that **cat. 10** indeed shows higher activity than **cat. 8**. This can be attributed to the lower impurities on the catalyst surface generated by the protecting shell. However, the expected doubling inactivity as a result of lowering the protective shell concentration to half its initial value did not materialize. As shown in Fig. 8, much scope for improvement is found compared with the conventional catalyst preparation based on tetraalkylammonium borate.

CONCLUSIONS

The *in situ* generation of excess protecting agent (NR_4Cl) in the $NR_4(BEt_3H)$ reduction method of colloidal nanoparticles synthesis can be reduced considerably without losing control over the particle size and composition. It was found that the optimum amount of NR_4Cl required to stabilize platinum and PtRu particles can be decreased by 40% when the required amount of BEt_3H^- reductant is substituted with $LiBEt_3H$.

Further, it was found that the reverse addition mode yields small nanoparticles with a narrow size distribution because of the homogeneous diffusional growth of nanoparticles. This mode reduces the cost of nanoparticles synthesis. Further, an enhancement in the methanol oxidation activity of the PtRu catalyst reflects a cleaner nanoparticle surface.

Acknowledgements

We sincerely want to thank Dr C. Weidenthaler and Mr B. Spliethoff, from Max-Planck-Institut für Kohlenforschung, for XRD and TEM measurements respectively. We also gratefully acknowledge the financial support by the Deutsche Forschungsgemeinschaft under grant no. BO 1135/2-5 (Priority program Fuel Cells).

REFERENCES

1. Turkevich J, Stevenson PC, Hillier J. *Disc. Faraday Soc.* 1951; **11**: 55.
2. Schmid G. *Clusters and Colloids*. VCH: Weinheim, 1994.
3. Bönnemann H, Brijoux W, Brinkmann R, Fretzen R, Joussen T, Köppler R, Neiteler P, Richter J. *J. Mol. Catal.* 1994; **86**: 129.
4. Bönnemann H, Braun G, Brijoux W, Brinkmann R, Tilling AS, Seevogel K, Siepen K. *J. Organometal. Chem.* 1996; **520**: 143.
5. Bönnemann H, Nagabhushana KS. In *Encyclopedia of Nanoscience and Nanotechnology*, vol. 1, Nalwa HS (ed.). American Scientific Publishers: 2004; 777.
6. Bönnemann H, Brijoux W. In *Active Metals*, Fürstner A (ed.). VCH: Weinheim, 1996; 339.
7. Bönnemann H, Brijoux W. In *Advanced Catalysts and Nanostructured Materials*, Moser W (ed.). Academic Press: 1996; 165.
8. Bönnemann H, Nagabhushana KS. In *Encyclopedia of Nanoscience and Nanotechnology*, Marcel Dekker: 2004; 739.
9. Bucher S, Hormes J, Modrow H, Brinkmann R, Waldöfner N, Bönnemann H, Beuermann L, Krischok S, Maus-Friedrichs W, Kempter V. *Surf. Sci.* 2002; **497**: 321.
10. Bönnemann H, Endruschat U, Hormes J, Köhl E, Kruse S, Modrow H, Mörtel R, Nagabhushana KS. *Fuel Cells* 2004; **4**: 1.
11. Wang ZL, Petroski JM, Green TC, El-Sayed MA. *J. Phys. Chem. B* 1998; **102**: 6145.
12. Schmidt TJ, Paulus UA, Gasteiger HA, Behm RJ. *J. Electroanal. Chem.* 2000; **508**: 41.
13. Goia DV, Matijević E. *New. J. Chem.* 1998; 1203.
14. Cao G. *Nanostructures and Nanomaterials*. Imperial College Press: 2004; chapter 3.
15. Schmidt TJ, Noeske M, Gasteiger HA, Behm RJ, Britz P, Bönnemann H. *J. Electrochem. Soc.* 1998; **145**: 925.
16. Schmidt TJ, Noeske M, Gasteiger HA, Behm RJ, Britz P, Bönnemann H. *Langmuir* 1997; **13**: 2591.
17. Bönnemann H, Richards RM. *Eur. J. Inorg. Chem.* 2001; 2455.
18. Schmid G. *Chem. Rev.* 1992; **92**: 1709.

19. Roucoux A, Schulz J, Patin H. *Chem. Rev.* 2002; **102**: 3757.
20. Bönnemann H, Brinkmann R, Britz P, Endruschat U, Mörtel R, Paulus UA, Feldmeyer GJ, Schmidt TJ, Gasteiger HA, Behm RJ. *J. New Mater. Electrochem. Syst.* 2000; **3**: 1999.
21. Paulus UA, Endruschat U, Feldmeyer GJ, Schmidt TJ, Bönnemann H, Behm RJ. *J. Catal.* 2000; **195**: 383.
22. Bönnemann H, Brinkmann R, Brijoux W, Dinjus E, Joussen Th, Korall B. *Angew. Chem.* 1991; **103**: 1344.